Physica A 390 (2011) 535–540

Contents lists available at ScienceDirect

Physica A

journal homepage: www.elsevier.com/locate/physa

Electron wave packet dynamics in twisted nonlinear ladders with correlated disorder

F.A.B.F. de Moura [a,*], U.L. Fulco [b,c], M.L. Lyra [a], F. Domínguez-Adame [d], E.L. Albuquerque [b]

[a] Instituto de Física, Universidade Federal de Alagoas, Maceió AL 57072-970, Brazil
[b] Departamento de Biofísica e Farmacologia, Universidade Federal do Rio Grande do Norte, 59072-970, Natal-RN, Brazil
[c] Departamento de Física, Universidade Federal do Ceará, 60455-760 Fortaleza-CE, Brazil
[d] Departamento de Física de Materiales, Universidad Complutense, E-28040 Madrid, Spain

ARTICLE INFO

Article history:
Received 29 July 2010
Received in revised form 15 September 2010
Available online 20 October 2010

Keywords:
Anderson Transition
Localization
Electrons
Transport
Correlated
Disorder

ABSTRACT

Within a tight-binding Hamiltonian approach, we study the dynamics of one-electron wave packets in a twisted ladder geometry with adiabatic electron–phonon interaction. The electron–phonon coupling is taken into account in the time-dependent Schrödinger equation through a cubic nonlinearity. This physical scenario incorporates several relevant ingredients to study the electronic wave packet dynamics in DNA-like segments. In the absence of nonlinearity, a random sequence of nucleotides pairs makes the wave packets remain localized, according to the standard picture of the Anderson localization. However, when the electron–phonon interaction is turned on, Anderson localization is suppressed and a subdiffusive regime takes place. Further, we show that the wave packet trapping can be controlled by an external field perpendicular to the helicity axis of the double-strand chain.

1. Introduction

The remarkable idea of using organic molecules for building electronic components can be traced back to 1974 [1]. Biological molecules have all the basic properties necessary for the assembly of nanoscale electronic devices [2]. They can transport electric current, transfer molecules from one location to another, and produce cascades that can be used for amplification of an optical or electronic signal. All of these properties can be applied to electronic switches, gates, storage devices, biosensors and biological transistors, to name just a few.

Specifically, the discovery that DNA can conduct an electrical current has made it an interesting candidate to overcome the limitations that classical silicon-based electronics is facing presently [3]. Although the binding of a single DNA molecule to an electrode is a tough job, and difficulties also arise in validating whether the two are actually connected, the effort pays off because DNA has been shown to act as an insulator [4,5], a semiconductor [6,7], a conductor [8], or even a proximity-induced superconductor depending on its sequence, length, orientation and environment [9]. Besides, individual DNA molecules are very suitable for producing a new range of devices that are much smaller, faster and more energy efficient that the present semiconductor-based one. In fact, DNA offers a solution to many of the hurdles that need to be overcome. It is one of the best nanowires in existence, and has the important properties to self-assemble and to self-replicate, making it possible to produce nanostructures with a precision that is not achievable with the classical silicon-based technologies [10]. Furthermore, although the long-range correlations could be responsible for the effective electronic transport at specific resonant energies of finite DNA segments, much of the anomalous spread of an initially localized electron wave packet can be accounted for by short-range pair correlations on DNA. This finding suggests that a systematic approach based on

* Corresponding author. Tel.: +55 82 3214 1429; fax: +55 82 3214 1645.
E-mail address: fidelis@if.ufal.br (F.A.B.F. de Moura).

0378-4371/$ – see front matter © 2010 Elsevier B.V. All rights reserved.
doi:10.1016/j.physa.2010.10.023

the inclusion of further short-range correlations on the nucleotide distribution can provide an adequate description of the electronic properties of DNA segments. Within the DNA transport properties context two formalisms are frequently used: *ab initio* calculations [5,11–14] and effective Hamiltonian models [15–23]. The *ab initio* formalism can provide detailed information about the electronic molecular levels and charge distribution. However it is currently limited to short molecules due to the large computational cost [23]. From the other side, effective Hamiltonian approaches, in spite of being much less detailed, allow for addressing systems of realistic lengths and can provide additional information regarding the long distance transport properties [15–26].

The presence of disorder in DNA-based molecules can be either due to their intrinsic nature (imperfections of the structures or random sequences of nucleotides) or could have originated from a random environment. Whenever disorder is involved, Anderson localization of quasiparticles states comes into play [27]. In three dimensions (3D), the states at the center of the quasiparticle band remain extended if the magnitude of the disorder is smaller than the bandwidth while the other states (in the neighborhood of the band edges) turn out to be exponentially localized. This implies the existence of two mobility edges, which separate the phase of extended states from the localized ones [28]. On the other hand, uncorrelated disorder of any magnitude causes localization of *all* one-particle eigenstates in one dimension (1D) [29] and two dimensions (2D) [30].

In low-dimensional systems, the effect of nonlinearity seems to be dominant over the role played by disorder. Considering a discrete nonlinear Schrödinger and quartic Klein–Gordon equations with disorder, it was proved that the second moment and the participation number of the wave packet do not diverge simultaneously [31,32]. The spreading of an initially localized wave packet in a 1D discrete nonlinear Schrödinger lattice with disorder was also recently studied, and it was observed that Anderson localization is suppressed and a subdiffusive dynamics takes place above a certain critical nonlinearity strength [33]. Moreover, analytical and numerical calculations for a reduced Fermi–Pasta–Ulam chain indicate that energy localization does not require more than one conserved quantity [34]. From the experimental point of view, investigations were made to clarify the interplay between disorder and nonlinearity, by means of the evolution of linear and nonlinear waves in coupled optical waveguides patterned on an AlGaAs substrate. It was also observed that nonlinear perturbations enhance localization of linear waves while inducing delocalization of the nonlinear ones [35].

The aim of this work is to push this field further by investigating the electronic wave packet dynamics in a twisted ladder geometry. Nonlinearity, disorder and correlations will be considered once these are particularly important for the description of DNA-like segments. A systematic *ab initio* study of the DNA conformational modes and their possible interactions with the electron motion was provided in Ref. [14]. The effective Hamiltonian for distinct kinds of DNA polarons was also presented. Here, we consider the electron–phonon interaction within the adiabatic approximation proposed in Refs. [36–40]. The effective third order electron–phonon contribution was pointed as a possible mechanism to breakdown the localization rules in disordered chains [33,39]. In addition, we study the competition between nonlinearity and a perpendicular electric field. Our results suggest that disordered ladder models, with a topology similar to effective Hamiltonian models of DNA molecules [15–23] display a diffusive-like spread of the electronic wave packet induced by nonlinearity. Further, we numerically demonstrate that this wave packet spreading is suppressed by an external electric field applied perpendicular to the ladder helicity axis.

2. Model and formalism

Our calculations make use of an adiabatic electron–phonon interaction within an effective nonlinear tight-binding model Hamiltonian describing an electron moving in a twisted ladder geometry with correlated disorder. This structure mimics the topology and the interstrand correlations presented in DNA segments. Considering a single orbital per site and nearest-neighbor interactions, the time dependent Schrödinger equation (with $\hbar = 1$) is given by [36,37]

$$\mathrm{i}\,\frac{\mathrm{d}\psi_{js}}{\mathrm{d}t} = \left(\epsilon_{js} + \chi|\psi_{js}|^2\right)\psi_{js} + V_{\parallel}\left(\psi_{j+1s} + \psi_{j-1s}\right) + V_{\perp}\psi_{j\bar{s}}. \tag{1}$$

Here $s = \pm 1$ labels each strand, and $\bar{s} = -s$ indicates the complementary one. The index $j = 1, \ldots, N$ runs over the sites along one of the strands, coupled by the hopping parameter $V_{\parallel}$. In the DNA molecule such hopping amplitude is effectively mediated by side chains of sugar-phosphate. Also, $V_{\perp}$ is the hopping parameter between complementary sites on each strand, and χ is the coupling constant of the local electron–phonon interaction.

We consider an electron initially localized at the orbital $|j_0\, s_0\rangle$, namely we take the initial condition $\psi_{js}(t=0) = \delta_{jj_0}\delta_{ss_0}$. We solved the set of nonlinear coupled differential equations using the tenth-order Adams–Bashforth–Moulton method initialized by the Dormand–Prince Runge–Kutta method of order eight with time step $\Delta t = 0.005$. The time step Δt was found to be enough to obtain accurate results for the parameter set used in the simulations. We are particularly interested in the square root of the mean-square displacement $\sigma(t)$ and the time-dependent participation function $\xi(t)$ defined by

$$\sigma(t) = \sqrt{\sum_{j,s}\left[(j-j_0)^2 + (s-s_0)^2\right]\,|\psi_{js}(t)|^2}, \tag{2}$$

$$\xi(t) = \left[\sum_{j,s}|\psi_{js}(t)|^4\right]^{-1}, \tag{3}$$

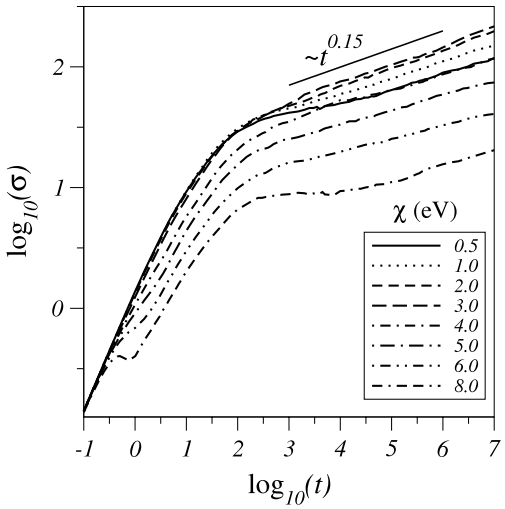

Fig. 1. Log–log plot of the square root of the mean-square displacement $\sigma(t)$ for several values of the nonlinear coupling constant χ. At long times $\sigma(t) \propto t^{0.15(2)}$, irrespective to the nonlinear strength.

as well as the return probability $R(t) = |\psi_{j_0 s_0}(t)|^2$. The participation function $\xi(t)$ gives an estimate of the number of sites over which the wave packet is spread at time t. In the long-time regime, its scaling behavior can also be used to distinguish between localized and delocalized wave packets. In addition, in a regime of strong localization, the probability of finding the particle at the initial site at long times $R_\infty \equiv \lim_{t\to\infty} R(t)$ is always nonzero [40].

We constructed uncorrelated random sequences containing four distinct values of the on-site potentials. In this sense, it mimics the sequence of four nucleotides present in DNA segments, namely adenine (A), guanine (G), thymine (T), and cytosine (C). Further, we considered the same fraction of each nucleotide found in the first sequenced human chromosome (Ch22), entitled NT_{011520}, whose number of nucleotides is about 3.4×10^6 [41]. For the on-site energies in one of the strands, we used the representative values: $\epsilon_A = 8.24$, $\epsilon_T = 9.14$, $\epsilon_C = 8.87$, and $\epsilon_G = 7.75$, all units in eV [42]. The energies of the other strand were generated by considering the interstrand nucleotide correlations which imposes that only base pairs CG and AT are allowed. In DNA molecules, the intrastrand hopping amplitude is smaller than the disorder width due to the variability of the on-site energies. The interstrand coupling mediated by the hydrogen bonds between complementary sequences is weaker than the intrastrand coupling. In order to reproduce some specific features of real DNA molecules, it would be important to consider both inter- and intra-strand hopping variability. Here we will concentrate on a tight-binding ladder model with $V_\parallel = 1.0$ eV and $V_\perp = 0.5$ eV. Although the following results were obtained for the above particular parameter set motivated by previous effective Hamiltonian descriptions of DNA-segments, the overall physical properties do not depend on a specific choice for the Hamiltonian parameters.

3. Results

We start with a wave packet localized at the guanine closer to the center of the double-strand molecule. In order to avoid finite-size effects, we used large segments with $N = 1.000$ base-pairs. We average the numerical calculations over 20 distinct segments to account for configurational variability. Fig. 1 shows the mean-square displacement $\sigma(t)$ for several values of the electron–phonon coupling constant χ. The values of $\log_{10}(\sigma)$ were averaged over 20 realizations of disorder. In the absence of nonlinearity ($\chi = 0$) the wave packet spreads over a segment of finite length. This is the well-defined Anderson localization regime in low-dimensional systems with uncorrelated disorder.

For nonlinear double-strand chains we observe a subdiffusive regime $\sigma \propto t^{0.15(2)}$. The exponent obtained here is in perfect agreement with the numerical calculations for 1D nonlinear chains with uncorrelated disorder [33]. However, we observe two distinct trends in the regime of weak and strong nonlinearities. For $\chi < 3$ eV, the wave packet width in the asymptotic sub-diffusive regime increases as χ is increased. On the other hand, a reverse trend sets up for stronger nonlinearities. Although the wave packet width remains subdiffusive in these two regimes, such nonmonotonic dependence on the nonlinearity points to distinct dynamical properties, as we will explore below.

In Fig. 2 we show the time dependence of the participation function $\xi(t)$ computed considering the same number $N = 1.000$ of base-pairs. The nonlinear coupling ranged from $\chi = 0.5$ up to 8 eV. As one can see, the wave packet displays a subdiffusive dynamics in the regime of weak nonlinear couplings ($\chi < 3$ eV), in which the time dependent participation function behaves like $\xi \propto (t)^{0.25(2)}$. However, the participation function remains finite in the regime of strong nonlinearities. Therefore the divergences of the wave packet width and participation number are not simultaneous. This feature had already been pointed out in disordered nonlinear systems [31]. Therefore, the regime of weak nonlinearity corresponds to a true delocalized phase for which the wave packet spatial extension diverges as the wave packet continuously spreads over the system. For strong nonlinearities, the wave packet extension remains finite although the second moment of the distribution

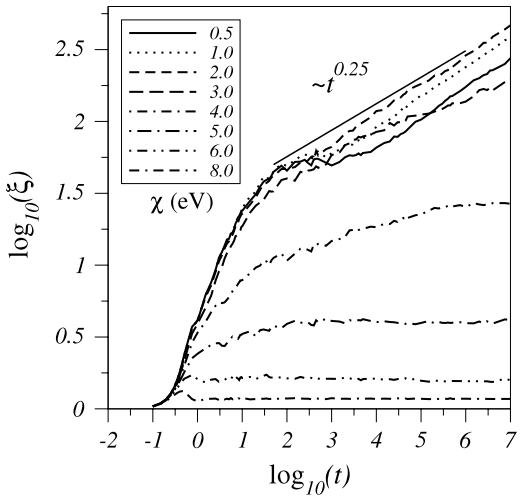

Fig. 2. Log–log plot of the time dependent participation function $\xi(t)$ for several values of the nonlinear coupling χ. At moderate electron–phonon couplings the participation function displays clear signatures of an asymptotic dynamics with $\xi(t) \propto t^{0.25(2)}$. For large couplings ($\chi > 3$ eV) the participation function saturates, thus indicating spatial localization of the wave packet.

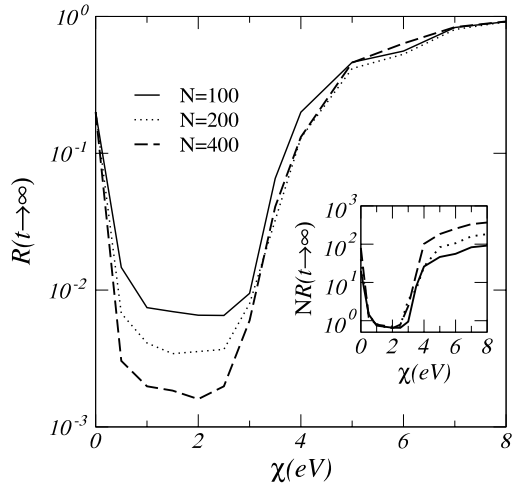

Fig. 3. Asymptotic return probability $Rt \to \infty$ as a function of the nonlinear coupling χ. For $0 < \chi < 2.5$–3.0 eV, the asymptotic return probability approaches zero as the system size increases, in agreement with the subdiffusive regime of the participation function shown in Fig. 2. For larger nonlinearities, the return probability remains finite and size independent. The inset shows the rescaled return probability NR_∞. The collapse of data at small nonlinearities signals the $1/N$ scaling of $R(t \to \infty)$ in the partially trapped regime.

continue to increase sub-diffusively. This feature is related to a partial self-trapping of the wave packet while the rest subdiffuses [32].

In order to have a more precise estimate of the critical nonlinearity delimiting the regimes of delocalized and partially self-trapped wave packets, we plot in Fig. 3 the return probability at very long times $Rt \to \infty$ versus the strength of the nonlinear coupling χ (after reflection at the chain boundaries). A clear transition is signaled at $\chi_c \simeq 2.5$–3.0 eV. Below χ_c the return probability decays as $1/N$ as stressed in the inset. For $\chi > \chi_c$ it becomes size independent. This result gives further support to the above claims, namely:

(i) For weak nonlinear couplings $\chi < \chi_c$, the asymptotic return probability $Rt \to \infty$ approaches zero, in agreement with the delocalized subdiffusive dynamics exhibited by both the wave packet width and participation function.
(ii) For strong nonlinear couplings $\chi > \chi_c$ we observe a localized regime $Rt \to \infty \neq 0$ corresponding to the self-trapping phenomenon already reported in 1D nonlinear chains. However, due to the subdiffusive growth of the wave packet width, such self-trapping is only partial [36,40].

Before finishing, we consider the effect of an external field $\mathcal{E}$ applied perpendicular to the ladder main axis. In this case, the helix conformation of the strands becomes important. This is equivalent to taking into account a gate voltage drop across the double helix. A 10-base-pair full-twist period will be considered which is similar to the one exhibited by the B form of the DNA. Neglecting the difference between major and minor grooves, the site energies under the gating electric field $\mathcal{E}$ will be: [23]

$$\widetilde{\epsilon}_{js} = \epsilon_{js} + Fs\cos(2\pi j/10), \tag{4}$$

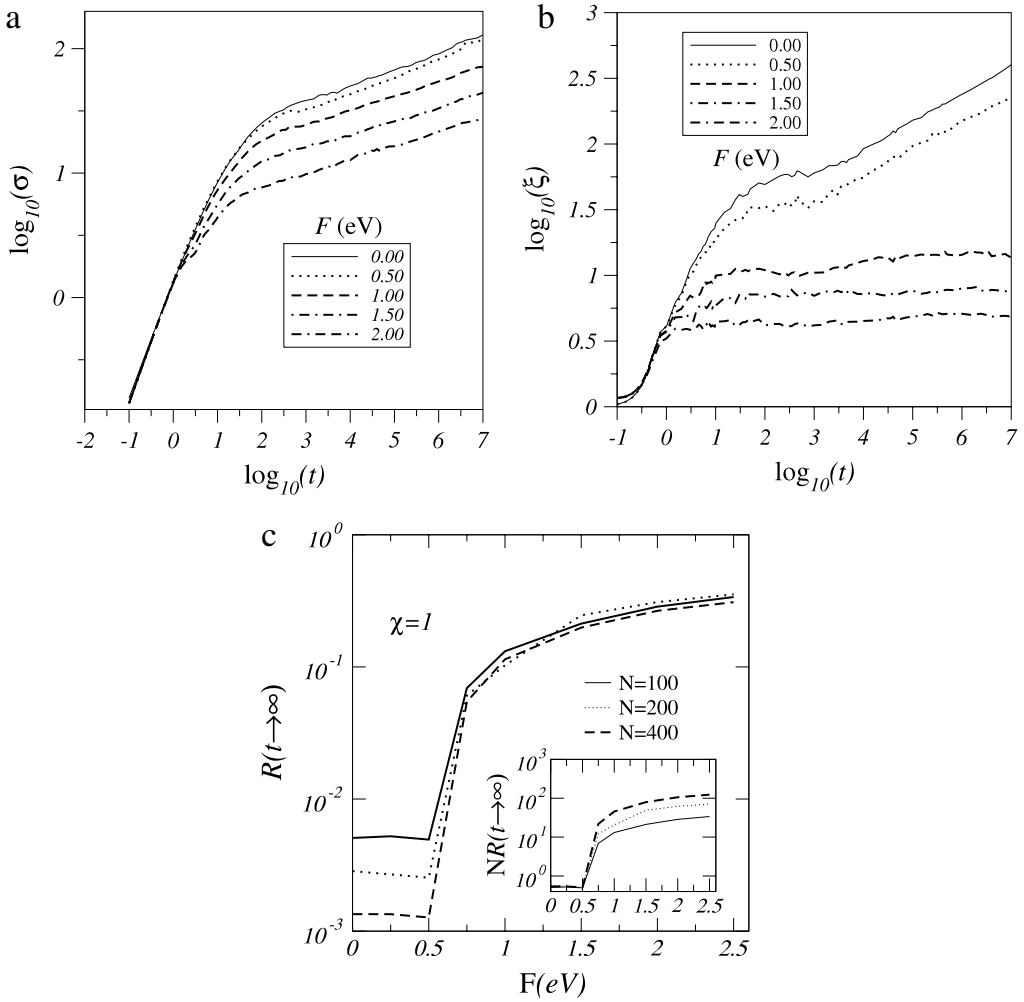

Fig. 4. (a) $\sigma(t)$ and (b) $\xi(t)$ as a function of time at $\chi = 1$ and several values of F, indicated on the labels. Notice that a partial self-trapping is attained at strong fields, signaled by the subdiffusive wave packet width spread together with a saturated participation function. (c) Asymptotic return probability $R(t \to \infty)$ versus F, indicating that the partial self-trapping takes place for fields $F > 0.5$ eV. The inset shows the scaled return probability NR_∞ which exhibits a data collapse in the delocalized regime.

with ϵ_{js} being the site energy at zero field. Also, F is the perpendicular gating energy, defined by $F \equiv e\mathcal{E}r$ where $r \sim 1$ nm is the strand radius. In Fig. 4(a) and (b) we plot the square root of the mean-square displacement $\sigma(t)$ and the time dependent participation function $\xi(t)$ as a function of time when the coupling constant of the local electron–phonon interaction $\chi = 1$ eV, for several values of F. For this value of χ the wave packet spreads continuously over the lattice in the absence of an external field, with both the wave packet width and participation function growing subdiffusively. The results show that the gating electric field reduces the wave packet spreading. However, the subdiffusive character of both wave packet width and participation function seems to remain for weak fields. This feature can be associated with the effective increase of the disorder width introduced by the perpendicular external field. On the other hand, the external field has a strong impact in the self-trapping phenomenon. Fig. 4(b) clearly shows that the participation function saturates at stronger fields even though the wave packet width still keeps its subdiffusive character. Fig. 4(c) depicts the asymptotic return probability versus F. While the return probability vanishes in the absence of the external field, a finite fraction of the electronic wave packet becomes trapped on its initial location when the perpendicular external field exceeds a critical value of the order of $F_c = 0.5$ eV. The fraction of the electronic density that becomes trapped increases as the electric field is increased.

4. Conclusions

In summary, we studied the dynamics of an electron wave packet in a double-stranded chain with a random sequence of on-site potentials and a cubic nonlinearity associated with an adiabatic electron–phonon interaction. By using the discrete nonlinear Schrödinger equation we include the influence of the lattice vibrations on the electron dynamics. To incorporate some ingredients of DNA-like segments, we considered a random four-valued sequence of on-site energies to mimic adenine, guanine, thymine, and cytosine nucleotides. The energies of the second strand were generated by considering the interstrand nucleotide correlations, which imposes that only base pairs CG and AT are allowed. We followed the time evolution of an electron initially localized at a single guanine orbital. In the absence of nonlinearity the system shows a well defined

Anderson localization regime. However, when the electron–phonon coupling is turned on, a subdiffusive regime arises in the regime of small nonlinearities and the electronic wave packet completely escapes from its initial location. In the regime of strong nonlinearities, a partial self-trapping emerges. In this regime a finite portion of the wave packet remains trapped near its initial position while the other part spreads subdiffusively. In addition, we consider the helix conformation of the ladder under the influence of a perpendicular gating field. Our calculations indicate that the electric field reduces the wave packet spreading. Actually, the external field is also able to trap a finite fraction of the electronic density near its initial location, a phenomenon that is controlled by the intensity of the external perpendicular field. It is important to stress that field-controlled devices play a mayor role in conventional electronics. The mechanism reported here for trapping electrons in helical double-strands opens the possibility of tailoring new field-controlled nanoscale bio-electronic devices. We hope that the present work will stimulate further studies on the transport properties in ladder geometries and the interplay of nonlinearity, geometry and field-effects.

Acknowledgements

This work was partially financed by the Brazilian Research Agencies CAPES (PROCAD, Rede NanoBioestruturas), CNPq (INCT-Nano(Bio)Simes, Project no. 573925/2008–9) and FAPERN/CNPq (Pronex). Work at Madrid was supported by MEC (projects Mosaico and MAT2010-17180).

References

[1] A. Aviram, M.A. Ratner, Chem. Phys. Lett. 29 (1974) 277.
[2] M.W. Shinwari, M.J. Deen, E.B. Starikov, G. Cuniberti, Adv. Funct. Mater. 20 (2010) 1865.
[3] D. Porath, A. Bezryadin, S. De Vries, C. Dekker, Nature 403 (2000) 635.
[4] E. Braun, Y. Eichen, U. Sivan, G. Ben-Yoseph, Nature 391 (1998) 775.
[5] P.J. De Pablo, F. Moreno-Herrero, J. Colchero, J.G. Herrero, P. Herrero, A.M. Baro, P. Ordejon, J.M. Soler, E. Artacho, Phys. Rev. Lett. 85 (2000) 4992.
[6] L.T. Cai, H. Tabata, T. Kawai, Appl. Phys. Lett. 77 (2000) 3105.
[7] A. Rakitin, P. Aich, C. Papadopoulos, Y. Kobzar, A.S. Vedeneev, J.S. Lee, J.M. Xu, Phys. Rev. Lett. 86 (2001) 3670.
[8] A.Y. Kasumov, M. Kociak, S. Gueron, B. Reulet, V.T. Volkov, D.V. Klinov, H. Bouchiat, Science 291 (2001) 280.
[9] M. Taniguchi, T. Kawai, Phys. Rev. E 70 (2007) 11913.
[10] E. Winfree, F. Liu, L.A. Wenzler, N.C. Seeman, Nature 394 (1998) 539.
[11] E.B. Starikov, Phil. Mag. Lett. 83 (2003) 699.
[12] H. Wang, J.P. Lewis, O.F. Sankey, Phys. Rev. Lett. 93 (2004) 016401.
[13] A. Hübsch, R.G. Endres, D.L. Cox, R.R.P. Singh, Phys. Rev. Lett. 94 (2005) 178102.
[14] E.B. Starikov, Phil. Mag. 85 (2005) 3435.
[15] E. Macia, S. Roche, Nanotechnology 17 (2006) 3002.
[16] S. Roche, D. Bicout, E. Macia, E. Kats, Phys. Rev. Lett. 91 (2003) 228101.
[17] S. Roche, Phys. Rev. Lett. 91 (2003) 108101.
[18] R. Gutierrez, R.A. Caetano, P.B. Woiczikowski, T. Kubar, M. Elstner, G. Cuniberti, New J. Phys. 12 (2010) 023022.
[19] D.A. Ryndyk, E. Shapir, D. Porath, A. Calzolari, R. Di Felice, G. Cuniberti, ACS Nano 3 (2009) 1651.
[20] R. Gutierrez, R.A. Caetano, B.P. Woiczikowski, T. Kubar, M. Elstner, G. Cuniberti, Phys. Rev. Lett. 102 (2009) 208102.
[21] R. Gutierrez, S. Mandal, G. Cuniberti, Phys. Rev. B 71 (2005) 235116.
[22] D. Klotsa, R.A. Römer, M.S. Turner, Biophys. J. 89 (2005) 2187.
[23] A.V. Malyshev, Phys. Rev. Lett. 98 (2007) 096801.
[24] E.L. Albuquerque, M.S. Vasconcelos, M.L. Lyra, F.A.B.F. de Moura, Phys. Rev. E 71 (2005) 021910.
[25] E.L. Albuquerque, M.L. Lyra, F.A.B.F. de Moura, Physica A 370 (2006) 625.
[26] F.A.B.F. de Moura, M.L. Lyra, E.L. Albuquerque, J. Phys.: Condens. Matter 20 (2008) 075109.
[27] P.W. Anderson, Phys. Rev. 109 (1958) 1492.
[28] N.F. Mott, J. Non-Cryst. Solids 1 (1968) 1.
[29] N. Mott, W.D. Twose, Adv. Phys. 10 (1961) 107.
[30] E. Abrahams, P.W. Anderson, D.C. Licciardello, T.V. Ramakrishnan, Phys. Rev. Lett. 42 (1979) 673.
[31] G. Kopidakis, S. Komineas, S. Flach, S. Aubry, Phys. Rev. Lett. 100 (2008) 084103.
[32] Ch. Skokos, D.O. Krimer, S. Komineas, S. Flach, Phys. Rev. E 79 (2009) 056211.
[33] A.S. Pikovsky, D.L. Shepelyansky, Phys. Rev. Lett. 100 (2008) 094101.
[34] D. Hajnal, R. Schilling, Phys. Rev. Lett. 101 (2008) 124101.
[35] Y. Lahini, A. Avidan, F. Pozzi, M. Sorel, R. Morandotti, D.N. Christodoulides, Y. Silberberg, Phys. Rev. Lett. 100 (2008) 013906.
[36] M. Johansson, M. Hörnquist, R. Riklund, Phys. Rev. B 52 (1995) 231.
[37] P.K. Datta, K. Kundu, Phys. Rev. B 53 (1996) 14929.
[38] F.A.B.F. de Moura, Iram Gléria, I.F. dos Santos, M.L. Lyra, Phys. Rev. Lett. 103 (2009) 096401.
[39] S. Flach, D.O. Krimer, C. Skokos, Phys. Rev. Lett. 102 (2009) 024101.
[40] Z. Pan, S. Xiong, C. Gong, Phys. Rev. E 56 (1997) 4744.
[41] The nucleotide sequence can be retrieved from the web page of the National Center of Biotechnology Information
[42] H. Sugiyama, I. Saito, J. Am. Chem. Soc. 118 (1996) 7063.